The Astronomical Journal, 153:61 (5pp), 2017 February doi:10.3847/1538-3881/153/2/61
© 2017. The American Astronomical Society. All rights reserved.

UKIRT MICROLENSING SURVEYS AS A PATHFINDER FOR *WFIRST*: THE DETECTION OF FIVE HIGHLY EXTINGUISHED LOW-|*b*| EVENTS

Y. Shvartzvald[1,7], G. Bryden[1], A. Gould[2,3,4], C. B. Henderson[1,7], S. B. Howell[5], and C. Beichman[6]
[1] Jet Propulsion Laboratory, California Institute of Technology, 4800 Oak Grove Drive, Pasadena, CA 91109, USA
[2] Max-Planck-Institute for Astronomy, Königstuhl 17, D-69117 Heidelberg, Germany
[3] Korea Astronomy and Space Science Institute, Daejon 305-348, Republic of Korea
[4] Department of Astronomy Ohio State University, 140 W. 18th Avenue, Columbus, OH 43210, USA
[5] Kepler & K2 Missions, NASA Ames Research Center, P.O. Box 1, M/S 244-30, Moffett Field, CA 94035, USA
[6] NASA Exoplanet Science Institute, California Institute of Technology, Pasadena, CA 91125, USA
Received 2016 October 11; revised 2016 November 30; accepted 2016 December 4; published 2017 January 10

ABSTRACT

Optical microlensing surveys are restricted from detecting events near the Galactic plane and center, where the event rate is thought to be the highest due to the high optical extinction of these fields. In the near-infrared (NIR), however, the lower extinction leads to a corresponding increase in event detections and is a primary driver for the wavelength coverage of the *WFIRST* microlensing survey. During the 2015 and 2016 bulge observing seasons, we conducted NIR microlensing surveys with UKIRT in conjunction with and in support of the *Spitzer* and *Kepler* microlensing campaigns. Here, we report on five highly extinguished ($A_H = 0.81$–1.97), low-Galactic latitude ($-0.98 \leqslant b \leqslant -0.36$) microlensing events discovered from our 2016 survey. Four of them were monitored with an hourly cadence by optical surveys but were not reported as discoveries, likely due to the high extinction. Our UKIRT surveys and suggested future NIR surveys enable the first measurement of the microlensing event rate in the NIR. This wavelength regime overlaps with the bandpass of the filter in which the *WFIRST* microlensing survey will conduct its highest-cadence observations, making this event rate derivation critically important for optimizing its yield.

Key words: Galaxy: bulge – gravitational lensing: micro

1. INTRODUCTION

In recent years, microlensing has established itself as an important technique for exoplanet detection and characterization. Since the first planet detected via microlensing over a decade ago (Bond et al. 2004), 43 exoplanets have been discovered in a variety of planetary systems and published,[8] including triple systems with one (e.g., Gould et al. 2014) or two (e.g., Gaudi et al. 2008) planets. Furthermore, microlensing is currently the only method that can systematically probe the free-floating planet population (Sumi et al. 2011). The ability of a microlensing experiment to detect these systems relies heavily on the underlying microlensing event rate, which mainly depends on the surface density of source and lens stars toward the survey fields. Therefore, microlensing surveys have concentrated their observing efforts toward the Galactic bulge, where the stellar surface density is highest. However, these surveys have been traditionally conducted in optical wavelengths, which suffer from high extinction near the Galactic plane and center, and thus their fields were selected in order to balance the stellar surface density with the extinction.

Extinction decreases as wavelength increases. Therefore, near-infrared (NIR; $>1\,\mu$m) microlensing surveys enable observations closer to the Galactic plane and center, where the event rate is expected to be higher (Gould 1995). Understanding this potential, the *WFIRST* flagship mission will conduct a 432 day NIR microlensing survey, divided equally into six 72 day seasons, toward the Galactic bulge (Spergel et al. 2015). This survey will revolutionize our understanding of bound planetary systems with separations of 1–10 au as well as free-floating exoplanets. However, until now no dedicated NIR microlensing surveys have been conducted, and so the event rate and the microlensing optical depth in the NIR have not been measured. VISTA Variables in the Vía Láctea (VVV) conducted a variability survey toward the inner Milky Way in the NIR, with multiple epochs in the K_s filter (Minniti et al. 2010). However, the survey cadence was irregular and too low to routinely detect microlensing events, which have a typical event timescale of $\sim$20 days. Currently, the VVV survey has published only one microlensing event (Minniti et al. 2015), which had a long timescale and was magnified for $\sim$100 days, and thus the VVV cadence was sufficient. This event was in a low-extinction field and was independently detected[9] in the *I*-band by the OGLE microlensing survey (Udalski et al. 2015).

NIR follow-up observations have been performed for microlensing events, usually in the *H*-band. These observations led to a measurement of the source flux in the observed NIR filters, a necessary component for the interpretation of post-event NIR adaptive optics (AO) observations. The AO observations resolve out stars not related to the event, isolating the microlensing target (source plus lens) and facilitating a measurement (or constraint) of the lens flux. This can break inherent degeneracies and enable a derivation of the physical properties of the lensing system, including its mass and distance.

In each of the last two bulge observing seasons, we conducted dedicated NIR microlensing surveys with UKIRT. These observations were carried out in conjunction with the space microlensing surveys performed with *Spitzer* (in 2015) and *K2* (in 2016). The UKIRT observations provided the NIR coverage required for future lens flux measurements as well as the cadence necessary for event detection and characterization. UKIRT observations were crucial for source characterization

[7] NASA Postdoctoral Program Fellow.
[8] As of 2016 November 30. From NASA Exoplanet Archive: http://exoplanetarchive.ipac.caltech.edu/.
[9] http://ogle.astrouw.edu.pl/ogle4/ews/ews.html

and anomaly coverage in the detection of a massive remnant in a wide binary (Shvartzvald et al. 2015). These surveys can also facilitate a preliminary estimation of the NIR event rate, although their total combined duration and area are currently not sufficient to constrain it precisely.

In this paper, we present the detection of five microlensing events discovered by the 2016 UKIRT survey, all of which are located in highly extinguished fields. These five detections are the result of an initial search for events within the 2016 UKIRT data set. As such, they emphasize the richness of the existing UKIRT microlensing survey data as well as the full potential that can be realized by a long-term NIR microlensing survey toward the inner bulge. In Section 2 we detail the observation and reduction procedures of our 2015–2016 surveys. In Section 3 we present the five new microlensing events and the extinction and reddening toward each, and set lower limits on the NIR event rate in our fields. Finally, we discuss the implications of these detections in Section 4.

2. OBSERVATIONAL DATA AND REDUCTION

The observations were carried out with the wide-field NIR camera (WFCAM) at the UKIRT 3.8 m telescope on Mauna Kea, Hawaii. The field of view of each of the four WFCAM detectors is $13.'6 \times 13.'6$ and the detector layout contains gaps with areas that are 94% of one detector. For a more detailed description of the instrument and telescope, see, e.g., Lawrence et al. (2007). All observations were in the *H*-band, with each epoch composed of sixteen 5 s co-added dithered exposures (2 co-adds, 2 jitter points, and 2×2 microsteps).

2.1. 2015 Northern Bulge Survey

In 2015 we conducted a 120 hr, 3.4 $\deg^2$ UKIRT survey in conjunction with the 2015 *Spitzer* microlensing campaign. Our survey focused on bulge fields north of the Galactic plane (see Figure 1), which suffer from high extinction. We thus complement the sparse optical coverage with higher-cadence, high signal-to-noise coverage in the NIR, enabling future lens flux measurements. Eighteen UKIRT fields were selected using the procedures developed by Poleski (2016), who showed that the product of the surface density of stars with $I < 20$ and clump stars is a good estimator of the microlensing event rate. The survey was conducted over 39 nights, spanning HJD′ (HJD–2450000) = 7180–7219, with a nominal cadence of five observations per night. During this period, 32 microlensing events discovered by OGLE were ongoing, and we recover the UKIRT light curve for all of them.

2.2. 2016 Southern Bulge Survey

In 2016, we carried out a second UKIRT survey, observing for 240 hr in conjunction with Campaign 9 of the *K*2 Mission (*K*2C9), which conducted the first automated microlensing survey from space (Henderson et al. 2016). The 2016 UKIRT survey supported the *K*2C9 survey, which observed toward the southern bulge, giving NIR coverage of events inside the survey superstamp. Thirty-two UKIRT fields were selected, covering 6.0 $\deg^2$, including the entire *K*2C9 superstamp and extending almost to the Galactic plane (see Figure 1). The survey was conducted over 91 nights, spanning HJD′ = 7487–7578, with a nominal cadence of two–three observations per night (limited by the bulge visibility at the beginning of the season).

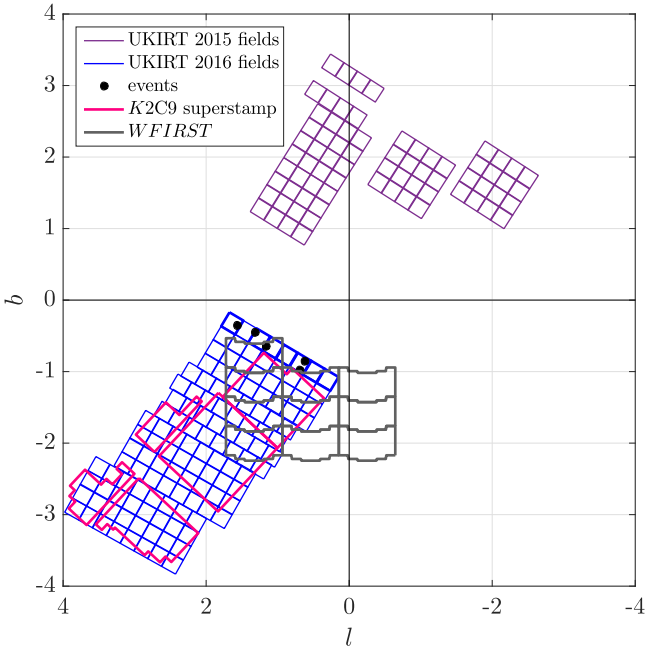

Figure 1. UKIRT 2015 (purple) and 2016 (blue) microlensing survey fields. Fields with thick lines are the seven 2016 fields searched in this work. The black circles are the positions of the detected events. Also shown are the *K*2C9 superstamp (pink) and the proposed *WFIRST* fields (gray).

2.3. Data Reduction

The UKIRT dithered images were reduced, astrometrically calibrated, and stacked by the Cambridge Astronomy Survey Unit (CASU; Irwin et al. 2004). Then, three different photometry methods were applied to the data in order to extract the light curves:

1. Multi-aperture photometry—standard 2MASS-calibrated photometry catalogs produced by CASU for all UKIRT/WFCAM images (Hodgkin et al. 2009). In the crowded fields of the Galactic bulge, this method works well only for bright (and/or completely isolated) stars, including partially saturated stars.
2. PSF photometry—using SExtractor (Bertin & Arnouts 1996) and PSFEx (Bertin 2011) and calibrated to 2MASS *H*-band magnitudes using comparison stars. This method works well even for crowded fields but not for saturated stars (thus making it complementary to method 1).
3. Difference image analysis (DIA) photometry—using the pySis software (Albrow et al. 2009). This method yields even better results for faint events and gives a smaller scatter than the first two methods. However, currently only the target DIA flux is measured, without photometric alignment to a standard system.

2.3.1. K2C9 Products

UKIRT light curves for all microlensing events detected within the *K*2C9 survey superstamp, whether by ground-based surveys and/or *K*2, will be uploaded to the *K*2C9 ExoFOP site.[10] Currently, only the light curves of known anomalous events (i.e., events for which the light curve deviates from that

[10] https://exofop.ipac.caltech.edu/k2/microlensing

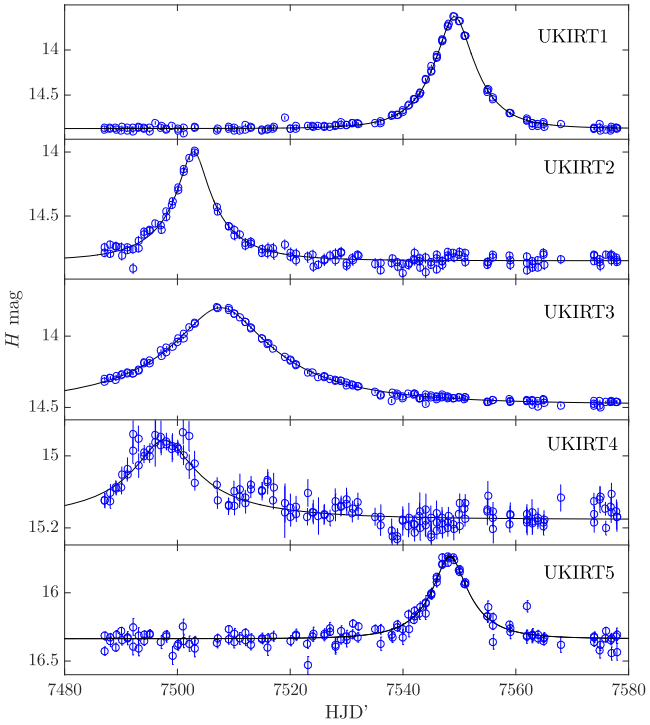

Figure 2. Light curves of the five UKIRT microlensing events.

expected for a single-lens microlensing event) have been uploaded to the website. Along with each light curve produced with methods 1 and 2, we also uploaded the photometric catalog of stars within 2′ of each microlensing target.

3. MICROLENSING EVENTS

3.1. Detections

The detection of a microlensing event is not a trivial task. Since the microlensing optical depth toward the Galactic bulge is $\mathcal{O}(10^{-6})$, millions of light curves need to be searched in order to detect an event. We applied a new event detection algorithm (D.-J. Kim et al. 2016, in preparation) that uses microlensing models calculated from a grid of times of peak magnification, t_0, and effective timescales, $t_{\rm eff} = t_{\rm E} \cdot u_0$ (where $t_{\rm E}$ and u_0 are the standard microlensing parameters; Paczynski 1986), to search for light curves characteristic of microlensing.

In this work we analyzed only 7 of the 128 subfields (each UKIRT field is composed of four subfields, corresponding to the four detectors) from the 2016 survey. We chose the seven subfields closest to the Galactic center, one of which is also the subfield closest to the Galactic plane. In total, we extracted 333,336 light curves for sources detected in at least 50 out of 152 epochs. We selected events for which t_0 occurs during the UKIRT survey and which also show a clear baseline. Here we present five new microlensing events, none of which were discovered by the optical microlensing surveys OGLE and MOA (Sumi et al. 2003), as indicated by their alert pages.[9,11] Figure 2 shows the light curves of these events, which we designate UKIRT1–5. In addition, we recovered three microlensing events that were independently detected and reported by OGLE (OGLE-2016-BLG-0262, OGLE-2016-BLG-0786, and OGLE-2016-BLG-1158).

[11] https://www.massey.ac.nz/~iabond/moa/alert2016/alert.php

Events UKIRT(2, 3, 4, 5) are located in OGLE-IV field 500 and were observed by OGLE with a ∼1 hr cadence, which nominally would be sufficient to detect them, given that their timescales are all $t_{\rm E} \gtrsim 7$ day, but for the extinction. UKIRT1, on the other hand, resides in OGLE-IV field 533, which is observed only occasionally.

3.2. Extinction and Reddening

A standard method to derive the extinction and reddening in Galactic bulge fields is by locating the position of Galactic red clump stars on a color–magnitude diagram (CMD) and comparing it to its intrinsic values (Yoo et al. 2004). The red clump is a well-populated and relatively isolated feature of Galactic bulge CMDs (Terndrup 1988; Stanek et al. 1994) due to the high stellar density in the bulge. Nataf et al. (2013) have thoroughly studied and developed this method, and measured the clump position and intrinsic properties of the Galactic bulge in OGLE fields.

We use VVV catalogs of stars within 2′ of each event to construct ($H - K_s$, H) CMDs (see Figure 3). We identify the red clump position in each CMD using the method developed by Nataf et al. (2013) and derive the extinction and reddening in each field by comparing these values to the intrinsic clump values. Specifically, the intrinsic clump color used is $(H - K_s)_{0,\rm cl} = 0.1$ and its $H_{0,\rm cl}$ magnitude slightly varies as a function of l, with $H_{0,\rm cl,GC} = 13.15$ at the Galactic center (Nataf et al. 2013). Table 1 gives, for each event, its equatorial and galactic coordinates, the intrinsic magnitude and instrumental position of the red clump, and the derived extinction and reddening.

UKIRT4 suffers from the highest extinction, with $A_H = 1.97$, while UKIRT5 has the lowest extinction, with $A_H = 0.81$. However, the event baseline magnitude for UKIRT5 is sufficiently faint ($H = 16.3$) that it was not detected in the optical. There are no publicly available deep optical catalogs of these fields that can be used to detect the red clump. Thus, the optical extinction cannot be measured directly. While a typical extinction ratio in the Galaxy is $A_I/A_H \sim 3.5$, this ratio can increase significantly for high extinctions and so sets only a lower limit on the optical extinction.

3.3. Models

A standard single-lens microlensing model with three "Paczyński" parameters, (t_0, $t_{\rm E}$, u_0), was fitted to each light curve, along with two additional flux parameters accounting for the source flux, f_s (which can be converted to the H-band source magnitude, H_s), and possible blend flux, f_b. As is common for single-lens events, we find a strong correlation between $t_{\rm E}$, u_0 and the blending fraction, defined as $f_{bl} = f_s/(f_s + f_b)$ (in this convention $f_{bl} = 1$ means no blending). Table 2 gives the best-fit model for each event. Since we had observations only with the H-band, we cannot derive the source color and thus its spectral type. Nevertheless, assuming the source is a bulge star, we estimate the source type based on its magnitude, H_s, relative to that of the red clump. This analysis suggests that the source of UKIRT1 is a clump star, the sources of UKIRT2–3 are red giant branch stars, and the sources of UKIRT4–5 are turn-off stars.

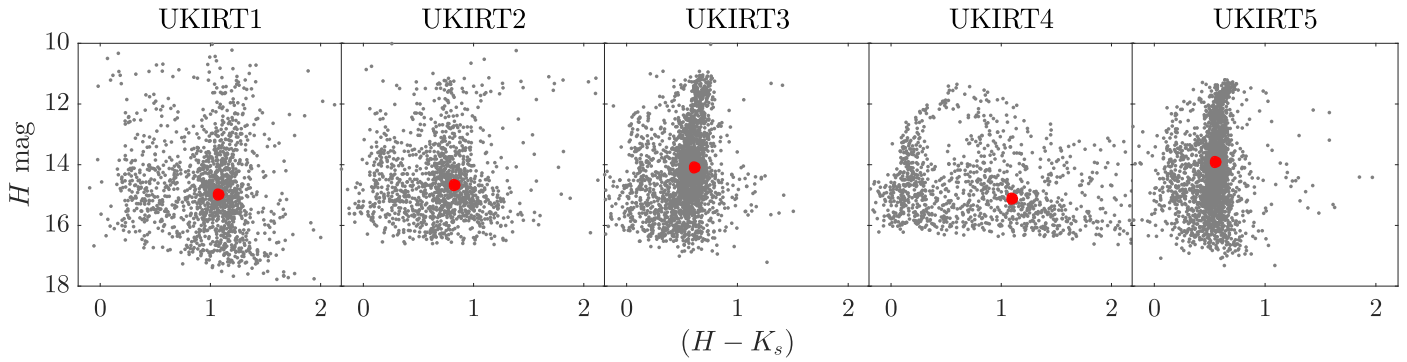

Figure 3. VVV color–magnitude diagrams (CMDs) for the fields of the five events. The red clump position for each is indicated by the red circle. The CMD for UKIRT4 emphasizes the high degree of differential reddening in this region.

3.4. NIR Event Rate

The frequency of microlensing events within the Galactic bulge varies considerably from field to field, depending on the Galactic structure along the line of sight. For large optical surveys, Monte Carlo simulations of the detection efficiency can be used to infer the underlying event rate (per star or per deg^2) and the optical depth (the fraction of sky filled by the Einstein rings of foreground lenses) for regions within a few degrees of the Galactic center (e.g., Sumi et al. 2013; Sumi & Penny 2016). While a detailed simulation of detection efficiency is not warranted by the small data set presented here, it is still worthwhile to consider the raw event rate within these fields, which reside in high-extinction regions for which the microlensing event rate has never before been measured.

From the number of events discovered, the total number of light curves, the area of the region analyzed in this work, and the survey duration, we are able to compute a preliminary estimate of the event rate in this subfields. Therefore, assuming perfect detection efficiency, our eight detections (five new events plus three detected by OGLE) from 333,336 light curves within the total area of 0.36 deg^2 of the seven subfields and a 91 day timespan give a rate of $96^{+47}_{-33} \times 10^{-6}$ events/star/year or 89^{+44}_{-31} events/deg^2/year. Given some inefficiency in our ability to detect all events, these estimates are lower limits on the true event rates.

Nevertheless, despite being conservative lower limits, these initial estimates for the microlensing event rate are in agreement with the Sumi & Penny (2016) results from the optical MOA survey. They found that the event rate increases toward the galactic plane (at longitudes $|l| < 5°$), until it becomes limited by the high extinction at midplane. While our NIR survey probes Galactic latitude $-1° < b < 0°$, they find peak rates at $b \approx -1.°5$ of $50^{+17}_{-13} \times 10^{-6}$ events/star/year and 90^{+15}_{-13} events/deg^2/year. Our uncorrected event rates are in agreement (and slightly exceed) the expected latitude dependent event rate found by Sumi & Penny (2016) of $[18.74 \pm 0.91] \times 10^{-6}$ exp$[(0.53 \pm 0.05)(3 - |b|)]$ events/star/year. While this high rate is of little value for optical surveys, the ideal target fields for *WFIRST*'s infrared survey may lie at relatively low-Galactic latitudes.

4. DISCUSSION

We present the first microlensing events detected from our 2016 UKIRT survey. This, along with our 2015 UKIRT survey, constitutes the first dedicated NIR microlensing program. The events were detected in highly extinguished fields and thus were not detected by optical microlensing surveys. These events are located close to the Galactic plane and center and give an indication of the NIR event rate in these fields, which is higher than that in the optical fields according to the preliminary lower limits we find. The 2015–2016 UKIRT fields are mostly overlapping with the optical microlensing surveys and thus will allow us, after analysis of our complete data set, to compare the number of events detected with UKIRT between different fields and give preliminary estimates of the relative event rate.

The *WFIRST* microlensing survey will primarily use a wide NIR filter in the range of 0.927–2.0 μm (Spergel et al. 2015). Our *H*-band UKIRT microlensing surveys are the first surveys conducted in a bandpass that overlaps with the highest-cadence filter of the *WFIRST* microlensing survey. The sources in our sample represent only the bright end of the source luminosity function and thus suggest that the NIR event rate in these fields will be high for *WFIRST*, given its expected photometric depth. All five events are at the edges of the currently proposed *WFIRST* fields (see Figure 1) and thus perhaps indicate that these fields should be moved even closer to the Galactic center.

Over 100 events detected by optical surveys and observed by *Spitzer* and *K*2C9 were ongoing during our UKIRT campaigns. For the vast majority of these, UKIRT observations will give H_s. This will allow for systematic AO follow-up observations of these targets in order to measure their lens fluxes and derive their physical properties. The lens flux method will be the primary channel for determining the physical properties of *WFIRST* microlensing planets (Yee 2015). The UKIRT sample can thus be used to help validate this technique using events with full characterization via the microlens parallax measurements from *Spitzer* and *Kepler*.

The relatively short duration of our experiments (39 and 91 days in 2015 and 2016, respectively) limited the number and types of events we can detect. While searching for events in this preliminary exploration of the UKIRT data, we found many light curves potentially indicative of microlensing events but for which the observations covered only the rising or falling portion of the light curve. In other cases, only the peak was observed, with no baseline data (suggestive of a long-timescale event, if indeed microlensing). Understanding these limitations and their implications for the detection efficiency of planets is important in the context of *WFIRST*, since each of its microlensing campaigns is planned to be 72 days long. Some of the event properties, in particular the validation that it is truly a microlensing event (and thus appears constant in other seasons), can be constrained using data from other seasons.

Table 1
Event Equatorial and Galactic Coordinates, Red Clump Intrinsic Magnitude $H_{0,\mathrm{cl}}$ and Instrumental Color and Magnitude $(H - K_s, H)_{\mathrm{cl}}$, Extinction, and Reddening

#	R.A. (J2000)	Decl. (J2000)	l (deg)	b (deg)	$H_{0,\mathrm{cl}}$ (mag)	$(H - K_s)_{\mathrm{cl}}$ (mag)	H_{cl} (mag)	A_H (mag)	$E(H - K_s)$ (mag)
1	17:50:40.9	−27:47:10.30	1.56	−0.36	13.09	1.07	15.00	1.91	0.97
2	17:50:26.5	−28:02:44.32	1.31	−0.45	13.10	0.83	14.65	1.55	0.73
3	17:50:50.9	−28:16:54.52	1.15	−0.64	13.11	0.62	14.10	0.99	0.52
4	17:50:24.6	−28:50:33.32	0.62	−0.85	13.13	1.10	15.10	1.97	1.00
5	17:51:05.3	−28:51:24.69	0.69	−0.98	13.12	0.55	13.93	0.81	0.45

Table 2
Best-fit Microlensing Model Parameters

#	t_0 (HJD′)	u_0	t_{E} (days)	H_s (mag)	f_{bl}	Source Type
1	7549.16	0.32	7.4	14.9	1.00	clump
2	7502.86	0.18	12.2	16.3	0.27	red giant branch
3	7507.70	0.24	28.5	15.9	0.27	red giant branch
4	7497.68	0.16	29.5	18.6	0.04	turn-off
5	7548.32	0.31	8.5	17.6	0.31	turn-off

Work by Y.S. and C.B.H. was supported by an appointment to the NASA Postdoctoral Program at the Jet Propulsion Laboratory, California Institute of Technology, administered by Universities Space Research Association through a contract with NASA. Work by A.G. was supported by NSF grant AST-1516842. The United Kingdom Infrared Telescope (UKIRT) is supported by NASA and operated under an agreement among the University of Hawaii, the University of Arizona, and Lockheed Martin Advanced Technology Center; operations are enabled through the cooperation of the Joint Astronomy Centre of the Science and Technology Facilities Council of the U.K. We acknowledge the support from NASA HQ for the UKIRT observations in connection with *K*2C9. Based on data products from observations made with ESO Telescopes at the La Silla Paranal Observatory under programme ID 179.B-2002.

REFERENCES

Albrow, M. D., Horne, K., Bramich, D. M., et al. 2009, MNRAS, 397, 2099
Bertin, E. 2011, in ASP Conf. Ser. 442, Astronomical Data Analysis Software and Systems XX, ed. I. N. Evans et al. (San Francisco, CA: ASP), 435
Bertin, E., & Arnouts, S. 1996, A&AS, 117, 393
Bond, I. A., Udalski, A., Jaroszyński, M., et al. 2004, ApJL, 606, L155
Gaudi, B. S., Bennett, D. P., Udalski, A., et al. 2008, Sci, 319, 927
Gould, A. 1995, ApJL, 446, L71
Gould, A., Udalski, A., Shin, I.-G., et al. 2014, Sci, 345, 46
Henderson, C. B., Penny, M., Street, R. A., et al. 2016, PASP, 128, 124401
Hodgkin, S. T., Irwin, M. J., Hewett, P. C., & Warren, S. J. 2009, MNRAS, 394, 675
Irwin, M. J., Lewis, J., Hodgkin, S., et al. 2004, Proc. SPIE, 5493, 411
Lawrence, A., Warren, S. J., Almaini, O., et al. 2007, MNRAS, 379, 1599
Minniti, D., Lucas, P. W., Emerson, J. P., et al. 2010, NewA, 15, 433
Minniti, D., Contreras Ramos, R., Alonso-García, J., et al. 2015, ApJL, 810, L20
Nataf, D. M., Gould, A., Fouqué, P., et al. 2013, ApJ, 769, 88
Paczynski, B. 1986, ApJ, 304, 1
Poleski, R. 2016, MNRAS, 455, 3656
Shvartzvald, Y., Udalski, A., Gould, A., et al. 2015, ApJ, 814, 111
Spergel, D., Gehrels, N., Baltay, C., et al. 2015, arXiv:1503.03757
Stanek, K. Z., Mateo, M., Udalski, A., et al. 1994, ApJL, 429, L73
Sumi, T., Abe, F., Bond, I. A., et al. 2003, ApJ, 591, 204
Sumi, T., Kamiya, K., Bennett, D. P., et al. 2011, Natur, 473, 349
Sumi, T., Bennett, D. P., Bond, I. A., et al. 2013, ApJ, 778, 150
Sumi, T., & Penny, M. T. 2016, ApJ, 827, 139
Terndrup, D. M. 1988, AJ, 96, 884
Udalski, A., Szymański, M. K., & Szymański, G. 2015, AcA, 65, 1
Yee, J. C. 2015, ApJL, 814, L11
Yoo, J., DePoy, D. L., Gal-Yam, A., et al. 2004, ApJ, 616, 1204